Journal of Hydrology 570 (2019) 304–314

Contents lists available at ScienceDirect

Journal of Hydrology

journal homepage: www.elsevier.com/locate/jhydrol

Research papers

The role of cross-correlation between precipitation and temperature in basin-scale simulations of hydrologic variables

S.B. Seo[a], R. Das Bhowmik[b,*], A. Sankarasubramanian[c], G. Mahinthakumar[c], M. Kumar[d]

[a] Institute of Engineering Research, Seoul National University, Seoul, South Korea
[b] Department of Civil Engineering, Indian Institute of Science, Bangalore, India
[c] Department of Civil, Construction, and Environmental Engineering, North Carolina State University, Raleigh, NC, USA
[d] Department of Civil, Construction, and Environmental Engineering, University of Alabama, Tuscaloosa, AL, USA

ARTICLE INFO

This manuscript was handled by Emmanouil Anagnostou, Editor-in-Chief, with the assistance of Qiang Zhang, Associate Editor

Keywords:
Cross-correlation
GCM
Univariate
Bias-correction
PIHM
Hydrologic simulation

ABSTRACT

Uncertainty in climate forcings causes significant uncertainty in estimating streamflow and other land-surface fluxes in hydrologic model simulations. Earlier studies primarily analyzed the importance of reproducing cross-correlation between precipitation and temperature (P-T cross-correlation) using various downscaling and weather generator schemes, leaving out how such biased estimates of P-T cross-correlation impact streamflow simulation and other hydrologic variables. The current study investigates the impacts of biased P-T cross-correlation on hydrologic variables using a fully coupled hydrologic model (Penn-state Integrated Hydrologic Model, PIHM). For this purpose, a synthetic weather generator was developed to generate multiple realizations of daily climate forcings for a specified P-T cross-correlation. Then, we analyzed how reproducing/neglecting P-T cross-correlation in climate forcings affect the accuracy of a hydrologic simulation. A total of 50 synthetic data sets of daily climate forcings with different P-T cross-correlation were forced into to estimate streamflow, soil moisture, and groundwater level under humid (Haw River basin in NC, USA) and arid (Lower Verde River basin in AZ, USA) hydroclimate settings. Results show that climate forcings reproducing the P-T cross-correlation yield lesser root mean square errors in simulated hydrologic variables (primarily on the sub-surface variables) as compared to climate forcings that neglect the P-T cross-correlation. Impacts of P-T cross-correlation on hydrologic simulations were remarkable to low flow and sub-surface variables whereas less significant to flow variables that exhibit higher variability. We found that hydrologic variables with lower internal variability (for example: groundwater and soil-moisture depth) are susceptible to the bias in P-T cross-correlation. These findings have potential implications in using univariate linear downscaling techniques to bias-correct GCM forcings, since univariate linear bias-correction techniques reproduce the GCM estimated P-T cross-correlation without correcting the bias in P-T cross-correlation.

1. Introduction

Precipitation (P) and temperature (T) are primary inputs for simulating streamflow using a hydrologic model. Depending on the watershed climate regime (e.g., arid/humid), streamflow is highly sensitive to uncertainties in climate forcings. Earlier studies on streamflow sensitivity have considered the changes in the moments of a single climate variable (Cai and Cowan, 2008; Kormos et al., 2016; Maurer and Duffy, 2005; Sankarasubramanian and Vogel, 2003; van Werkhoven et al., 2008; Vano et al., 2012; Zhang et al., 2014). However, the sensitivity of streamflow simulations/projections due to bias in the cross-correlation between precipitation and temperature (hereafter the P-T cross-correlation) arising from downscaling and disaggregation has rarely been addressed. This is a critical issue as most bias-corrected P and T from General Circulation Models (GCMs) (e.g., MACA – Abatzoglou and Brown, 2012; BOR – Reclamation, 2013) are based on univariate methods, which merely reproduce the raw P-T cross-correlation from GCMs (Das Bhowmik, 2016; Das Bhowmik et al., 2017). In this study, we systematically analyzed how biased estimates of the P-T cross-correlation influence the simulations of streamflow and other land-surface fluxes.

Studies have investigated the spatial variability in the P-T cross-correlation and the associated land-surface responses over the continental and global scale. Trenberth and Shea (2005) estimated the covariability of monthly mean surface P and T globally. They reported that the P-T cross-correlation is negative over the land during the

* Corresponding author.
E-mail address: rajarshidb@iisc.ac.in (R. Das Bhowmik).

https://doi.org/10.1016/j.jhydrol.2018.12.076
Received 15 October 2018; Received in revised form 19 December 2018; Accepted 30 December 2018
Available online 14 January 2019

summer, whereas, over the high latitudes, the cross-correlation is positive during the winter season. Zhao et al. (1993) also found that summer P and T are negatively correlated over most parts of the coterminous United States (CONUS), which indicates increased T resulting in reduced P. In Liu et al. (2012), evaluated the P-T cross-correlation from GCMs from Coupled Model Intercomparison Project Phase-5 (CMIP5) and found that responses of P-T cross-correlations from GCMs are 2–3 times smaller than the observed values. Das Bhowmik (2016) showed that the P-T cross-correlations from GCMs are not within the sampling variability of the observed P-T cross-correlation on 40–50% of grid points over the CONUS. A recent study has inspected the impact of ignoring the joint dependency between P and T on hydrologic simulation by applying a joint bias-correction on climate model outputs (Chen et al., 2018). They reported that the joint bias-correction performed better than the independent bias-correction to simulate streamflow on 11 out of 12 watersheds for the calibration period. However, the study relied on a single measure to reproduce the P-T cross-correlation and did not consider hydrologic fluxes other than the streamflow.

Hydrologic models calibrated with historical datasets are forced with climate model projections to predict the long-term changes in hydrologic fluxes. Watershed management, reservoir operation, water-supply planning, and design of hydraulic structures depend on the reliable estimation of non-stationarity in hydrologic variables (Hovenga et al., 2016; Šraj et al., 2016). Overall, climate outputs from more than 10 climate models are suggested to be considered as climate forcings to perform hydrological simulations/projections (Hosseinzadehtalaei et al., 2017). However, climate model outputs exhibit a high amount of model bias (on individual variables) and run on a spatial resolution different from the resolution of the hydrologic model (Das Bhowmik et al., 2017). Further, decadal predictions are reported to have initial model drift, i.e., model prediction shifts towards the model climatology instead of projecting based on the initialized conditions (Choudhury et al., 2017; Taylor et al., 2012). To summarize, hydrologic researchers could not force projections from climate models directly into the hydrologic model due to bias, a mismatch in spatial resolution, and model drift; therefore, climate model outputs requires processing before hydrologic modeling (Mazrooei et al., 2015; Seo et al., 2016).

Over the years, studies have suggested various pre-processing approaches for bias-correction, statistical downscaling, temporal disaggregation, and initial drift correction (Choudhury et al., 2017, Das Bhowmik et al., 2017; Prairie et al., 2007; Wilks and Wilby, 1999, Wood et al., 2004;). Researchers have assumed stationarity while applying pre-processing schemes on future projections (Johnson and Sharma, 2012). Pre-processing approaches follow a wide range of algorithms and techniques, from simple regression to complex weather generators (Huth, 1999; Sankarasubramanian and Lall, 2003; Stoner et al., 2012; Wilks and Wilby, 1999). For bias-correction, bias-correction and statistical downscaling (BCSD) (Wood et al., 2004) remains as a popular database for hydroclimate analyses. Under this, bias-correction is carried out for a single variable (for example, precipitation/temperature/relative humidity) at a time using simple regression or quantile mapping, which neglects the inter-dependence between multiple variables. However, besides the bias in the mean and the standard deviation of climate projections, climate models exhibit a substantial bias to reproduce the observed P-T cross-correlation under univariate linear bias correction (Das Bhowmik et al., 2017). In general, the observed P-T cross-correlations are statistically significant, and they exhibit large magnitudes. For example, during July, more than half of the total grid points across the CONUS witness statistically significant P-T cross-correlation. Previous studies have shown that univariate bias correction methods reproduce the GCM estimated P-T cross-correlation, thereby resulting in significant bias in the P-T cross-correlation (Das Bhowmik, 2016; Ivanov and Kotlarski, 2017; Wilcke et al., 2013). We assume that a substantial bias in the statistically significant P-T cross-correlation could potentially impact a hydrological simulation and the associated cross-correlation in land surface fluxes. Given that hydrological simulations/projections are obtained using a physical model, deriving an analytical relationship on how the bias in the P-T cross-correlation propagates through simulated hydrological variables is difficult. To the best of our knowledge, limited or no study systematically analyzes how biased estimate of the P-T cross-correlation impacts the hydrologic simulation.

This study's objective is to evaluate the importance of reproducing the P-T cross-correlation in climate forcings during hydrologic simulation. We investigate how neglecting the P-T cross-correlation in climate forcings affects the performance of hydrologic simulations. For this purpose, we investigated four hydrologic variables – streamflow, evapotranspiration, soil moisture depth, and groundwater level. To obtain different sets of P-T cross-correlation, a synthetic weather generator – which provides multiple realizations of daily climate forcings – was developed. Two ensembles of climate forcings were forced into a fully coupled hydrologic model (Penn-state Integrated Hydrological Model, PIHM) – out of which, one reproduced the observed P-T cross-correlation while the other neglected the observed P-T cross-correlation. Using the PIHM set up for two watersheds from humid and arid hydro-climatic regimes, simulated hydrologic variables from two different climate forcings were compared with the respective reference variables obtained using the observed climate forcings.

This manuscript is organized as follows: The next section presents details of the target basins, the hydrologic model, and data sets. Next, we discuss the experimental design. The results are presented in Section 4, which is followed by concluding remarks.

2. Background

2.1. Target basins

Two watersheds, Haw River in North Carolina (USGS − 03030002) and Lower Verde River in Arizona (USGS – 15060203), were considered to represent humid climate regime of southeastern US and arid climate regime of southwestern US, respectively. The Haw River is located in the eastern part of the US Sunbelt. The headwaters of the Haw River run 177 km into the Jordan Lake reservoir, and the drainage area of the basin is 3959 km^2, receiving a mean annual precipitation of 1131 mm (Seo et al., 2018a,b). The Lower Verde River, a part of the Lower Colorado River basin, covers approximately 5090 km^2 of central Arizona, receiving a mean annual precipitation of 474 mm. The spatial resolution of the observed P-T series is (1/8° × 1/8°). Using (1/8° × 1/8°) grid points, the observed monthly P-T cross-correlation was calculated and plotted for each grid point over the Haw River (Fig. 1a) and the Lower Verde River (Fig. 1b) basins for four seasons, JFM (January–March), AMJ (April–June), JAS (July–September), and OND (October–December). The Haw River basin experiences statistically significant negative P-T cross-correlations across all the grid points during AMJ and some grid points during JAS. On the other hand, the Lower Verde River basin exhibits statistically significant negative P-T cross-correlation across all the grid points during OND and some grid points during the other seasons. Statistical significance is based on 95% confidence interval following the equation $[\pm 1.96/\sqrt{(n-3)}]$ where n is the number of observations. Overall, both basins experience weak P-T cross-correlations during JFM, which is the wettest season of a year.

2.2. Hydrologic model and data sets

PIHM is used for the analyses. It is a fully distributed multi-process model in which surface water, groundwater, and land surface components are fully coupled using a semi-discrete finite volume approach (Kumar, 2009; Qu and Duffy, 2007).

Observed P-T data sets, daily observations at (1/8° × 1/8°) spatial resolution, were downloaded from Ed Maurer's research group (Maurer et al., 2002). Streamflow and groundwater datasets for the target basins

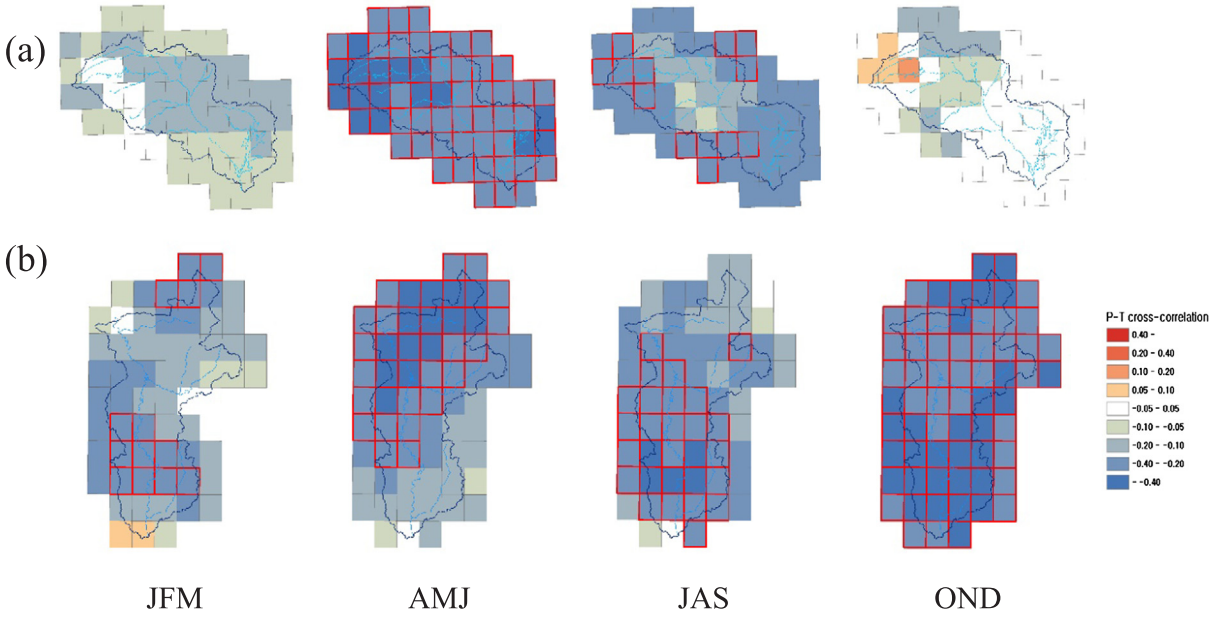

Fig. 1. Monthly P-T cross-correlation on each grid point for JFM (January–March), AMJ (April–June), JAS (July–September), and OND (October–December): (a) the Haw River basin (b) the Lower Verde River basin. Grid points with red boundary indicate that the observed P-T cross-correlation on the grid point is statistically significant at a 95% confidence interval. (For interpretation of the references to colour in this figure legend, the reader is referred to the web version of this article.)

were obtained from USGS Water Data webpage (USGS Water Data webpage, 2015). The two streamflow gauges are HCDN (Hydro-Climatic Data Network) stations, which are located in streams subjected to minimal anthropogenic influences, such as pumping or upstream storage (Sankarasubramanian et al., 2001; Vogel and Sankarasubramanian, 2000).

Seo et al. (2016) calibrated PIHM parameters for the Haw River and the Lower Verde River basins using the observed P-T time series. The current study uses the same calibrated model for the Haw River basin and the Lower Verde River basin. Table 1 presented calibration and validation results for the target basins. Correlation values for the streamflow during calibration and validation periods are higher than 0.9 (0.8) for the Haw River (Lower Verde River). PIHM exhibits a higher NSE value for streamflow during the September-October-November season as compared to other seasons, which resulted from PIHM's ability to model high flow values during fall months. Correlation and NSE values related to the groundwater are slightly lower than the values related to the streamflow. Nevertheless, PIHM shows a consistent performance for a long-term simulation of streamflow and groundwater across different seasons for both rivers.

3. Experimental design

3.1. Synthetic P-T generator

GCM forcings obtained using univariate linear bias-correction methods reproduce the raw P-T cross-correlation from GCMs, which are significantly biased compared to the observed P-T correlation for the historical period (Das Bhowmik, 2016; Das Bhowmik et al., 2017). Note that univariate linear bias-correction methods reproduce the moments, mean, and standard deviation of the forcings, but it can provide biased estimates of P-T cross-correlation. Hence, it is essential to understand how biased P-T cross-correlation from univariate bias-correction methods could impact the streamflow simulations/projections under potential climate change. To demonstrate this, we employ a synthetic P-T generator that develops two sets of time-series of P and T having different P-T cross-correlation. The first set reproduces the observed P-T cross-correlation and individual moments (mean and standard deviation), while the second set does not preserve the observed P-T cross-correlation but reproduces only the mean and standard deviation of P-T series. These two sets of forcings with different P-T cross-correlation are provided as inputs to the PIHM to understand the importance of reproducing the P-T cross-correlation.

Table 1
Evaluation of the model performance for each season: correlation Coefficient and Nash-Sutcliffe Efficiency values of monthly streamflow and GW depth for each target basin (Seo et al., 2016).

	Watershed	Station Name/Number	Calibration (1956–1980)							Validation (1981–2005)								
			CC				NSE				CC				NSE			
			DJF	MAM	JJA	SON	DJF	MAM	JJA	SON	DJF	MAM	JJA	SON	DJF	MAM	JJA	SON
Streamflow	Haw River	At Haw River	0.95	0.93	0.94	0.97	0.84	0.82	0.86	0.92	0.94	0.86	0.88	0.94	0.77	0.74	0.73	0.86
	Verde River	Above Horseshoe dam	0.89	0.79	0.89	0.89	0.74	0.61	0.73	0.78	0.80	0.92	0.90	0.92	0.53	0.65	0.80	0.85
Groundwater	Haw River	USGS 355522079043001	0.82	0.80	0.77	0.77	0.63	0.59	0.56	0.57	0.70	0.69	0.68	0.67	0.48	0.47	0.45	0.45
	Verde River[1)]	USGS 341408111212901	0.79					0.54										

1) Calibration periods of Verde River groundwater level are 1978–1985 due to lack of data length.

3.1.1. Reproducing covariance structure of monthly P-T series

A multivariate log-normal distribution function is used to generate multiple realizations of P-T series for the specified (i.e., observed or biased) P-T cross-correlation. First, spatially averaged monthly P-T series on each target basin is developed. Subsequently, synthetically generated P-T series is spatially disaggregated over all the grid points of the target basins. Detailed steps of the proposed synthetic generator are listed as follows:

1) Based on log-transformed P and T datasets, estimate the mean monthly P and T, $\bar{M}$ [1 × 24], vector and the covariance matrix, $\bar{C}$ [24 × 24], of spatially averaged monthly mean P-T series from observed monthly P-T series (1951–2010). For both the mean vector and the covariance matrix, index values 1–12 represent P from January to December, and index values 13 to 24 represent T from January to December. The covariance matrix specifies both the variance, auto-covariance between different lags and the P-T cross-covariance.
2) Revise the observed covariance matrix, $\bar{C}$, so that the matrix only contains the standard deviations of P and T, the co-variability between P-T, and the lag-1 auto-correlation of T (i.e., the other values in the matrix become zero). The elements of the revised covariance matrix, $\bar{C}^{pres}$[24 × 24], is given below, with i and j being the number of the row and the column, respectively. Fig. S1 in the supporting information illustrates the matrix form of $\bar{C}^{pres}$[24 × 24].

$$\bar{C}^{pres}(i,\ j) = E[(P_i - \mu_{P_i})(P_i - \mu_{P_i})]\ when\ i = j \le 12$$
$$= E[(T_{i-12} - \mu_{T_{i-12}})(T_{i-12} - \mu_{T_{i-12}})]\ when\ i = j \ge 13$$
$$= E[(T_{i-12} - \mu_{T_{i-12}})(T_{j-12} - \mu_{T_{j-12}})]\ when\ i \ge 13,\ j \ge 13,$$
$$and\ |i - j| = 1$$
$$= E[(P_{i-12} - \mu_{P_{i-12}})(T_{i-12} - \mu_{T_{i-12}})]\ when\ i \ge 13\ and\ (i - j) = 1$$
$$= E[(P_{j-12} - \mu_{P_{j-12}})(T_{j-12} - \mu_{T_{j-12}})]\ when\ j \ge 13\ and\ (j - i) = 1$$
$$= o,\ otherwise$$

3) Generate monthly P-T series $\bar{F}_i^{pres}$ for the i^{th} year, assuming a multivariate log-normal distribution with the mean vector and the revised covariance matrix: i.e.

$$\bar{F}_i^{pres} \sim mvnrnd(\bar{M},\ \bar{C}^{pres}) \quad (1)$$

4) Iterate step 3 until total n (n = 60) years of monthly P-T series are generated.

Hereafter, the cross-correlation between the spatially averaged P-T is referred to as the synthetic-average P-T cross-correlation. We implement the following steps to generate a synthetic P-T time series that ignores the covariance structure:

5) Revise the covariance matrix, $\bar{C}$, so that the matrix only contains the variances of P and T and the lag-1 correlation of T. In this, we explicitly assume no cross-covariance between P-T. The elements of the revised covariance matrix $\bar{C}^{non-pres}$, [24 × 24], is given below, with i and j being the number of the row and the column, respectively. Fig. S2 in the supporting information illustrates the matrix form of $\bar{C}^{non-pres}$[24 × 24].

$$\bar{C}^{non-pres}(i,\ j) = E[(P_i - \mu_{P_i})(P_i - \mu_{P_i})]\ when\ \ i = j \le 12$$
$$= E[(T_{i-12} - \mu_{T_{i-12}})(T_{i-12} - \mu_{T_{i-12}})]\ when\ \ i = j \ge 13$$
$$= E[(T_{i-12} - \mu_{T_{i-12}})(T_{j-12} - \mu_{T_{j-12}})]\ when\ \ i \ge 13,$$
$$j \ge 13\ \ and\ \ |i - j| = 1$$
$$= 0,\ \ otherwise$$

6) Repeat step 3 and 4 to generate monthly P-T series with no covariance: i.e.,

$$\bar{F}_i^{non-pres} \sim mvnrnd(\bar{M},\ \bar{C}^{non-pres}) \quad (2)$$

3.1.2. Reproducing spatial dependence on the local scale

Once spatially averaged monthly P-T series is generated, we disaggregate the spatially averaged series over each grid point of the target basins. Spatial noise for each grid point is estimated as the mean deviance to the spatial mean value. Detailed steps of spatial noise generator have been listed as follows:

1) Estimate covariance matrix of deviation of monthly P (T) to the spatial mean P (T) for the j^{th} month, SC_j^P (SC_j^T) [m × m], where m is the total number of grids. We obtain total 24 covariance matrices for each month of P and T.
2) Generate spatial noise of P (T) on each grid for the j^{th} month in the i^{th} year, $SN_{i,j}^P$ ($SN_{i,j}^T$), from a multivariate log-normal distribution with a zero-mean vector, O [1 × m], and the covariance matrix of P (T) obtained in step 1 for each month.

$$SN_{i,j}^P \sim\ mvnrnd(O,\ SC_J^P) \quad (3a)$$

$$SN_{i,j}^T \sim mvnrnd(O,\ SC_J^T) \quad (3b)$$

3) Iterate step 3 until total n (n = 60) years of time series are generated.
4) Obtain the final values ($P_{i,j,k}^{pres}$, $P_{i,j,k}^{non-pres}$, $T_{i,j,k}^{pres}$, and $T_{i,j,k}^{non-pres}$) that are monthly P series reproducing observed P-T cross-correlation, monthly P series without observed P-T cross-correlation, monthly T series reproducing observed P-T cross-correlation, and monthly T series without observed P-T cross-correlation, respectively, for the k^{th} grid of the j^{th} month in the i^{th} year, by adding generated spatial noise on each grid: i.e.,

$$P_{i,j,k}^{pres} = \bar{F}_{i,j}^{pres} + SN_{i,j,k}^P \quad (4a)$$

$$P_{i,j,k}^{non-pres} = \bar{F}_{i,j}^{non-pres} + SN_{i,j,k}^P \quad (4b)$$

$$T_{i,j,k}^{pres} = \bar{F}_{i,j+12}^{pres} + SN_{i,j,k}^T \quad (4c)$$

$$T_{i,j,k}^{non-pres} = \bar{F}_{i,j+12}^{non-pres} + SN_{i,j,k}^T \quad (4d)$$

After this, a set of P-T series that reproduce the observed P-T cross-correlation is referred as Opt 1, and a set of P-T series without observed P-T cross-correlation is referred as Opt 2. We refer the cross-correlation between the spatially disaggregated P and T as the synthetic-disaggregated P-T cross-correlation.

3.2. Hydrologic simulation

Two different sets of hydrologic variables are simulated by forcing two synthetic data sets of monthly P-T series (Opt 1 and Opt 2) into the PIHM. Before hydrologic simulation, the monthly P-T series are temporally disaggregated into daily series Prairie et al.'s (2007) approach. Performances from the two different synthetic P-T series are evaluated by comparing the accuracy in simulating monthly hydrologic variables.

4. Results

4.1. Synthetic P-T series

We estimated the synthetic-average P-T cross-correlation for the Haw River (Fig. 2a) and the Lower Verde River basins (Fig. 2b). Square markers represent the observed P-T cross-correlation over the target basins. Triangle and asterisk markers show the median value of the synthetic-average P-T cross-correlation from Opt 1 and Opt 2, respectively. The grey envelope exhibits the range (i.e., the distance between

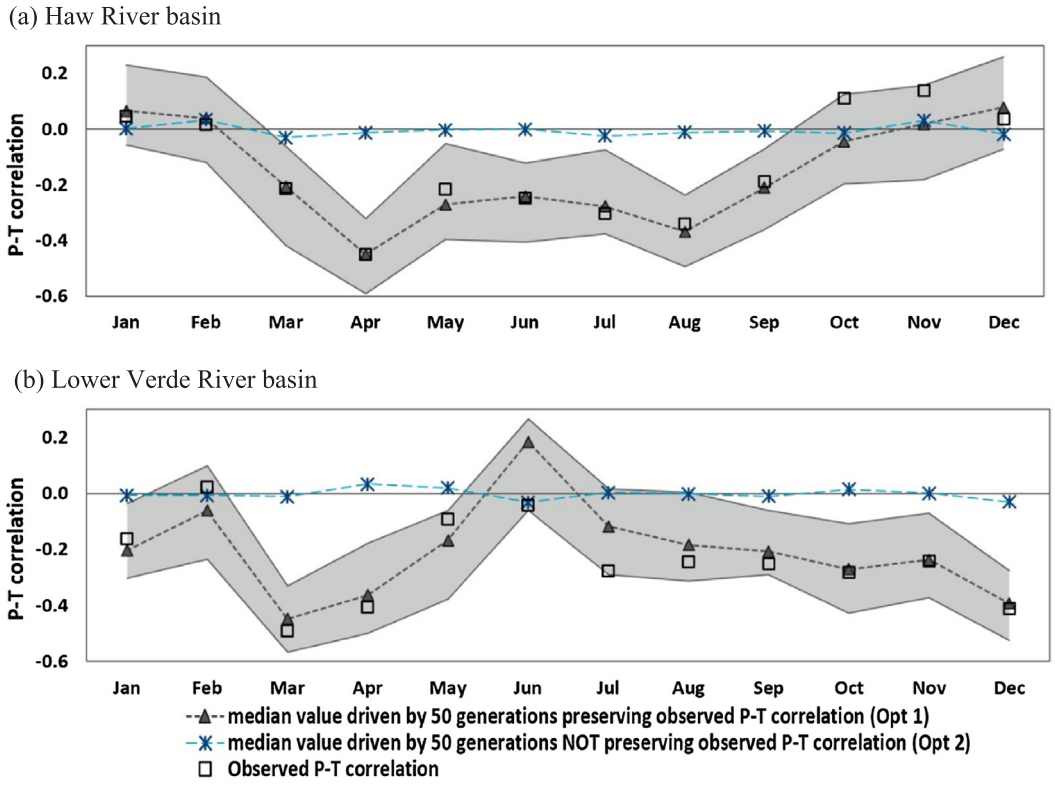

Fig. 2. P-T cross-correlation estimated by the spatially averaged monthly P-T series: (a) the Haw River basin and (b) the Lower Verde River basin. The monthly P-T series is generated, following the synthetic generator approach (sub-section 2.3.1). Grey envelope represents the range of P-T cross-correlations estimated by Opt 1 (i.e., the range between the maximum and the minimum).

the maximum and minimum values) of multiple sets of the synthetic-average P-T cross-correlation values from Opt 1. The observed P-T cross-correlations were reproduced by Opt 1 for the Haw River basin (Fig. 2a) for most months. The observed P-T cross-correlations for October and November were positive but statistically insignificant. Hence, Opt 1 failed to yield the observed P-T cross-correlation during October and November. Synthetic time series for the Lower Verde River basin reproduced the observed P-T cross-correlation across all months (Fig. 2b), except July. Based on this, we infer that Opt 1 reproduces the observed P-T cross-correlation in the synthetic climate forcings. Since Opt 2 neglects the observed P-T cross-correlation during the synthetic generation process, the synthetic-average P-T cross-correlations from Opt 2 were close to zero.

Subsequently, we generated the synthetic-disaggregated P-T cross-correlations for April over the Haw River (Fig. 3a) and the Lower Verde River basins (Fig. 3b). The results for April were presented as an example since the observed P-T cross-correlations during April are statistically significant for both river basins. Maps on the left-hand side show the observed P-T cross-correlations, whereas the maps in the middle (the right-hand side) present median (one randomly selected sample) of the synthetic-disaggregated P-T cross-correlations. Total 50 realizations were generated for Opt 1, and the synthetic-disaggregated P-T cross-correlations were produced for each realization. We found that the spatial dependence of the observed P-T cross-correlations is reproduced during the disaggregation process, although the synthetic-disaggregated P-T cross-correlation values are slightly higher for the northern grid points (Fig. 3a). Spatial variability of the synthetic-disaggregated P-T cross-correlation becomes high to low as we move from the median to the sample map. For the Lower Verde River basin (Fig. 3b), the spatial dependence of the observed P-T cross-correlations is efficiently reproduced in the synthetic-disaggregated P-T cross-correlation across the grid points (the median and the sample maps). In conclusion, Opt 1 efficiently reproduces the spatial dependence of the observed P-T data sets.

4.2. Simulation of hydrologic variables

Mean monthly values of the hydrologic variables (streamflow, 10th percentile of streamflow, 90th percentile of streamflow, soil moisture depth, and groundwater level) were obtained from the PIHM simulation. Observed P-T series was forced with the PIHM to obtain the reference simulation of the hydrologic variables. The reference simulation is used later to compare the performance of the model under synthetic climate forcings: Opt 1 and Opt2. We estimated the root mean square error (RMSE) for the reference simulation as well as 50 realizations of the simulated variables to quantify the impact of biased P-T cross-correlation in simulating/projecting hydrologic variables.

4.2.1. Simulation of streamflow variables

Differences in RMSE of mean monthly streamflow variables between Opt 1 and Opt 2 are presented for the Haw River basin (Fig. 4a–f) and the Lower Verde River basin (Fig. 4g–l). Negative differences (colored in red) in RMSE indicate Opt 1 performs better than Opt 2, since the simulated variables under Opt1 is closer (compared to Opt 2) to the simulated variables obtained with observed forcings. The grey lines represent the mean monthly values of the reference simulation driven by the observed P-T series (presented on the secondary axis). For the Haw River basin, as a whole, Opt 1 performs better than Opt 2 to simulate the mean monthly streamflow (Fig. 4a) for January to September. In case of the Lower Verde River basin, Opt1 outperforms Opt 2 in simulating the mean monthly streamflow for the fall and early winter (January) months (Fig. 4g). The observed P-T cross-correlations from April to August over the Haw River basin are statistically significant and witness negative values (Fig. 2a). However, the observed P-T cross-correlations from July to January for the Lower Verde River basin are statistically significant and have negative values (Fig. 2b). During

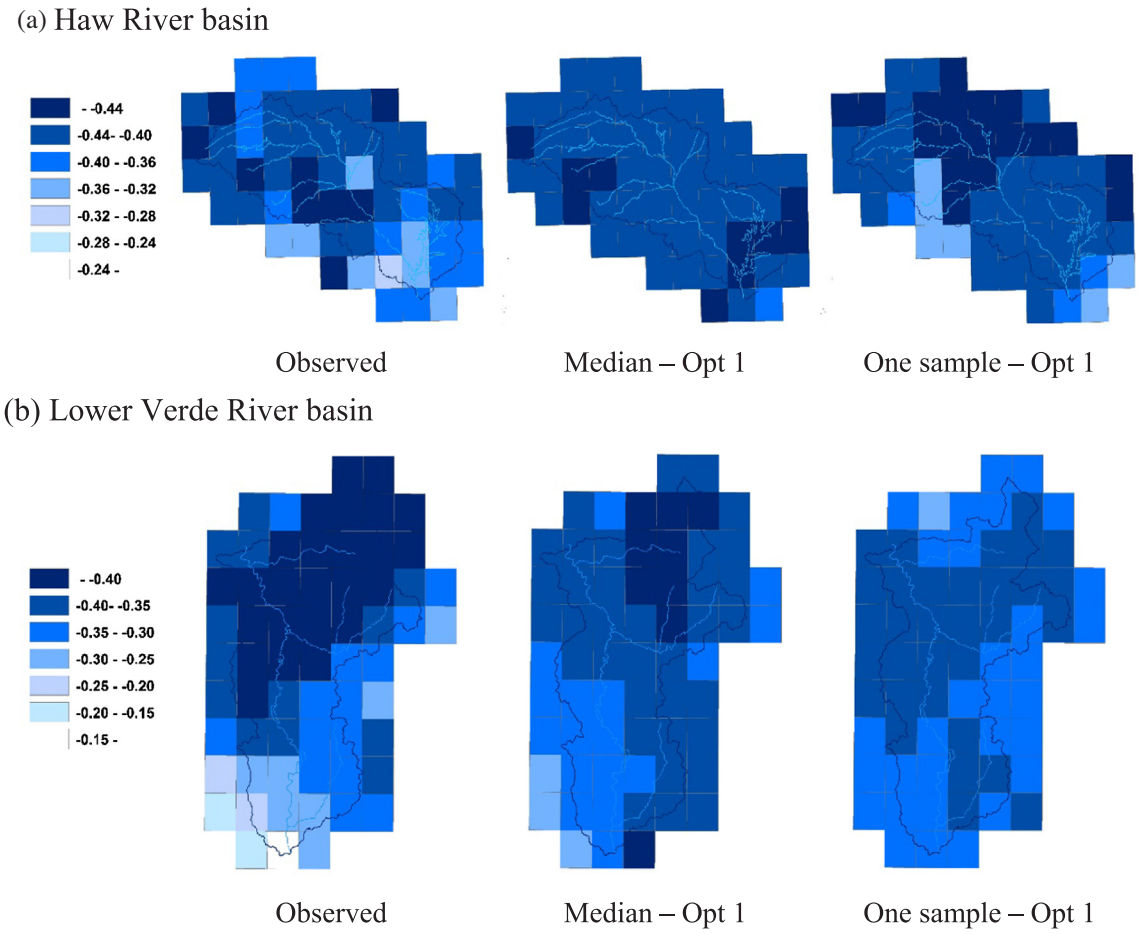

Fig. 3. Synthetic-disaggregated P-T cross-correlation on each grid point in April: (a) the Haw River basin and (b) the Lower Verde River basin.

statistically significant periods, Opt 1 performs better than Opt 2. Hence, our study finds that forcing the hydrologic model with unbiased estimates of the P-T cross-correlation results in an improved accuracy in the simulation of mean monthly streamflow.

Performance statistics related to streamflow extremes exhibit that Opt 1 performs better than Opt 2 with lower values of RMSE. A climate forcing that reproduces the observed P-T cross-correlation has a lower error variance in extreme flows simulations (7-day low, 10th percentile, 90th percentile, and 3-day peak streamflow) as compared to the forcing that does not reproduce the observed P-T cross-correlation. For the high extremes (90th percentile and 3-day peak), Opt 1 performs better than Opt 2 during almost all the months for the Haw and the Lower Verde River basins (Fig. 4e, 4f, k, and l), whereas Opt 1 performs better than Opt 2 for the low extreme (7-day low and 10th percentile) for the Haw River basin, especially during January and February. Additionally, for the Lower Verde basin, Opt 1 is better than Opt 2 to simulate the low flows during most months (Fig. 4h and i). Thus, reproducing the observed P-T cross-correlation improves the accuracy of streamflow simulation.

Fig. 5 presents percent differences in RMSE of streamflow between Opt 1 and Opt 2. Negative percent changes (blue colored gradient in Fig. 5) indicates better performance of Opt 1 than Opt 2. In general, Opt 1 outperforms than Opt 2 to reduce the error in estimating the streamflow. For Haw River basin, with the exception of few months, the RMSE to simulate the streamflow under Opt 1 is lower than the RMSE under Opt 2 for almost all the months. On the other hand, for the Lower Verde River basin, the RMSE of Opt 1 is consistently lesser than the RMSE of Opt 2 for all flow conditions except during July. Even though Opt 2 performs slightly better than Opt 1 during summer months, the differences in the estimated mean values of different flow attributes are very small. Fig. 4 shows the actual values of mean monthly flow attributes for the two schemes over the selected basins. It must be noted that both basins experience negative P-T cross-correlations during the summer, which indicates that increased moisture availability is associated with decreased temperature. Hence, any misspecification of the P-T cross-correlation is expected to have larger impact on the evapotranspiration as compared to the streamflow, since the evapotranspiration is the significant land-surface loss runoff during the summer. Overall, the analyses presented in Figs. 4 and 5 show that reproducing the P-T cross-correlation is important to estimate the observed streamflow.

4.2.2. Simulation of sub-surface water variables

Fig. 6a–c (6d and 6f) present differences in RMSE in simulating surface/sub-surface hydrologic variables, mean monthly evapotranspiration (ET), soil moisture depth (SM), and groundwater level (GW), respectively, for the Haw River basin (Lower Verde River basin). In general, climate forcings that reproduce the observed P-T cross-correlation (Opt 1) simulate the surface/sub-surface variables substantially better than climate forcings that neglect the observed P-T cross-correlation (i.e., Opt 2). For the Haw River basins, Opt 1 outperforms Opt 2 during dry seasons for ET simulation (Fig. 6a). SM simulation over the Haw River basin (Fig. 6b) was improved by the observed P-T cross-correlation across all months, except for the winter months (November to January). Similarly, Opt 1 is superior to Opt 2 to simulate the GW of the Haw River basin across all months except October (Fig. 6c). Considering all months, Opt 1 performs better than Opt 2 for the Haw River basin. For the Lower Verde River basin, Opt 1 exhibits lower errors than Opt 2 to simulate all the surface/sub-surface hydrologic variables (Fig. 6d–f) across all the months. The differences

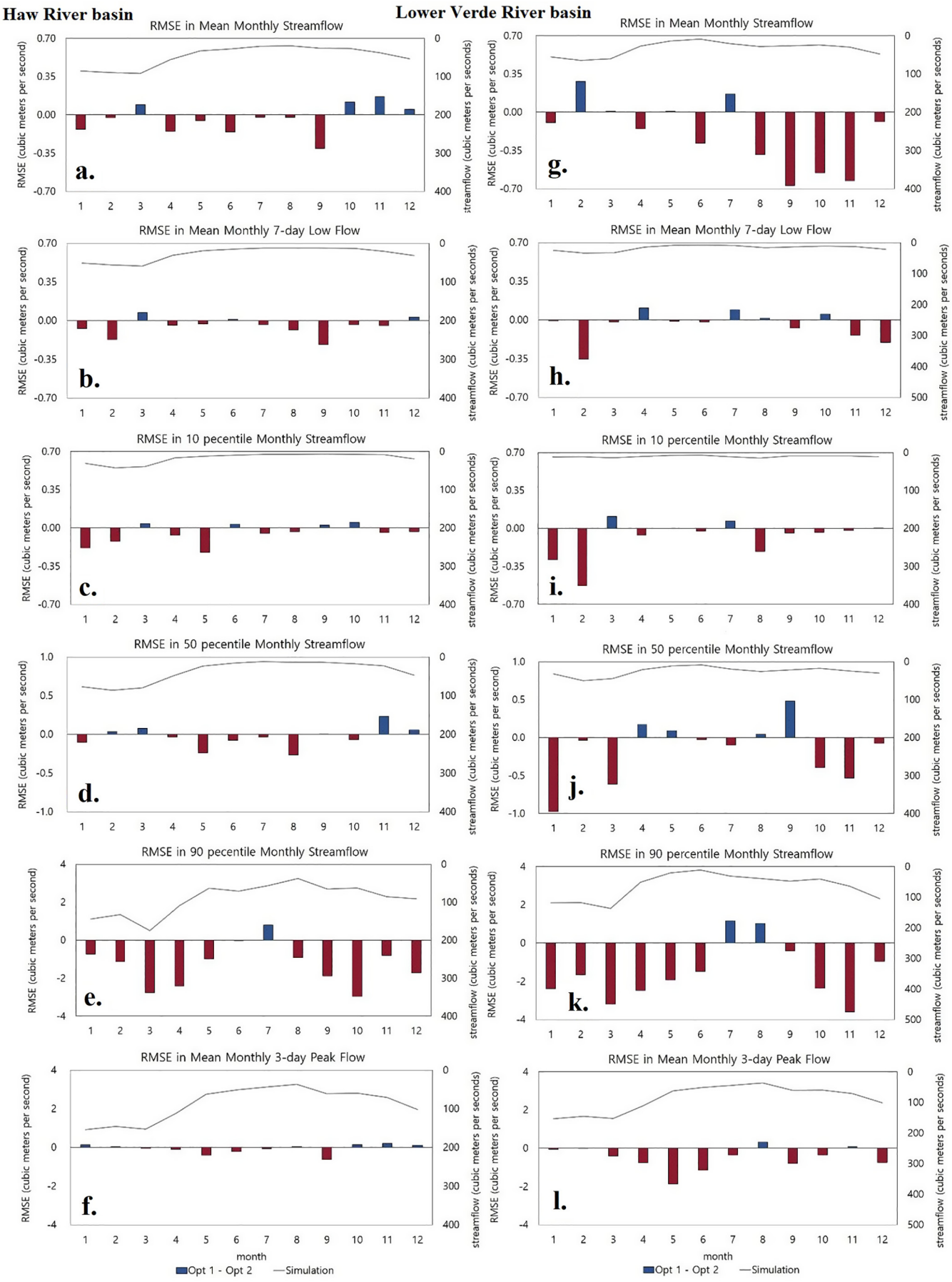

(caption on next page)

Fig. 4. Differences in RMSE of streamflow variables between Opt 1 and Opt 2 (i.e., RMSE of Opt 1 – RMSE of Opt 2). Mean monthly values of the reference simulation is presented on the secondary axis. (a) Haw River basin – mean monthly streamflow; (b) Haw River basin – mean monthly 7-day low streamflow; (c) Haw River basin – 10 percentile monthly streamflow; (d) Haw River basin – 50 percentile monthly streamflow; (e) Haw River basin – 90 percentile monthly streamflow; (f) Haw River basin – mean monthly 3-day peak streamflow; (g) Lower Verde River basin – mean monthly streamflow; (h) Lower Verde River basin – mean monthly 7-day low streamflow; (i) Lower Verde River basin – 10 percentile monthly streamflow; (j) Lower Verde River basin – 50 percentile monthly streamflow; (k) Lower Verde River basin – 90 percentile monthly streamflow; and (l) Lower Verde River basin – mean monthly 3-day peak streamflow.

in RMSE for both river basins were higher in magnitude during the summer and the fall months as compared to the rest of the year. It must be noted that during the summer and fall months, the observed P-T cross-correlations have exhibited statistical significance for the Haw and Lower Verde River basins (Fig. 2a and b). Hence, we infer that the impact of the P-T cross-correlation is more prominent on the surface/sub-surface hydrologic variables as compared to the streamflow variables. Our results show that a surface/sub-surface hydrologic variable is more sensitive to the negative P-T cross-correlation if the inter-annual variability of the variable is lower.

Fig. 7 presents percent differences in RMSE of surface/sub-surface hydrologic variables between Opt 1 and Opt 2 to cut off marginal improvement in the results. Notably, for the Haw River basin, Opt 1 led to a substantial improvement in sub-surface variables, SM and GW, from May to September where significant negative P-T cross-correlation exists. Since the amount of ET becomes significant during the summer season, GW typically becomes shallow with low SM. The impact of a negative P-T cross-correlation on either surface/sub-surface variables or streamflow increases during the summer months. Thus, inaccurate P-T cross-correlation in the forcing dataset would result in an accurate estimation of land-surface fluxes.

5. Concluding remarks

The current study evaluated the role of the P-T cross-correlation in basin-scale simulations of hydrologic variables for two watersheds representing arid and humid climate regime. Two sets of synthetic P-T time series were generated, where one reproduced the observed P-T cross-correlation and the other did not have any P-T correlation. These two synthetic P-T time series were forced into a fully-coupled hydrologic model to evaluate the impact of the P-T cross-correlation on hydrologic simulations. We found that climate forcing that reproduces the observed P-T cross-correlation reduce errors in simulated streamflow and sub-surface hydrologic variables as compared to the climate forcing that neglects the observed P-T cross-correlation. The performance metric – the difference in RMSE between Opt 1 and Opt 2 – were substantial for the months when the observed P-T cross-correlations are statistically significant. The reproduction of the observed P-T cross-correlation resulted in lower errors in the surface/sub-surface hydrologic variables in comparison to the streamflow variables, since the inter-annual variability of surface/sub-surface variables is smaller than the inter-annual variability of streamflow. We expect that a hydrologic simulation with correlated climate variables should impact the dependency among hydrologic variables with storage dampening the dependency on the climate variables.

This study's primary finding is that the simulation of a hydrologic variable using a forcing dataset that neglects the multivariate cross-correlation would lead to large bias in low flow values. It is important to reproduce the observed P-T cross-correlation in forcing data sets, especially during dry conditions when the observed P-T cross-correlation is negative. Therefore, appropriate estimation of the correlation between P-T is a critical factor for hydrologic extreme conditions, such as droughts. Additionally, impacts of reproducing the P-T cross-correlation on hydrologic simulations are more significant for surface/sub-surface variables than streamflow variables. It might be because of the fact that higher variability of streamflow variables attenuate the role of P-T cross-correlation. We conclude that reproducing the observed P-T correlation improves the simulation performance, especially when the P-T cross-correlation exhibits statistical significance.

The primary implications from the analyses indicate utilizing bias-corrected and downscaled GCM outputs for projecting streamflow and surface/sub-surface variables under climate change. It is well-known that GCM outputs require significant pre-processing schemes (e.g., bias-correction, downscaling, and drift correction) before forcing them into hydrologic models. Das Bhowmik (2016) reported that univariate bias-correction does not reproduce the observed P-T cross-correlation at a finer resolution of (1° × 1°). Since, GCM forcings from univariate bias-correction methods are typically forced into hydrologic models to

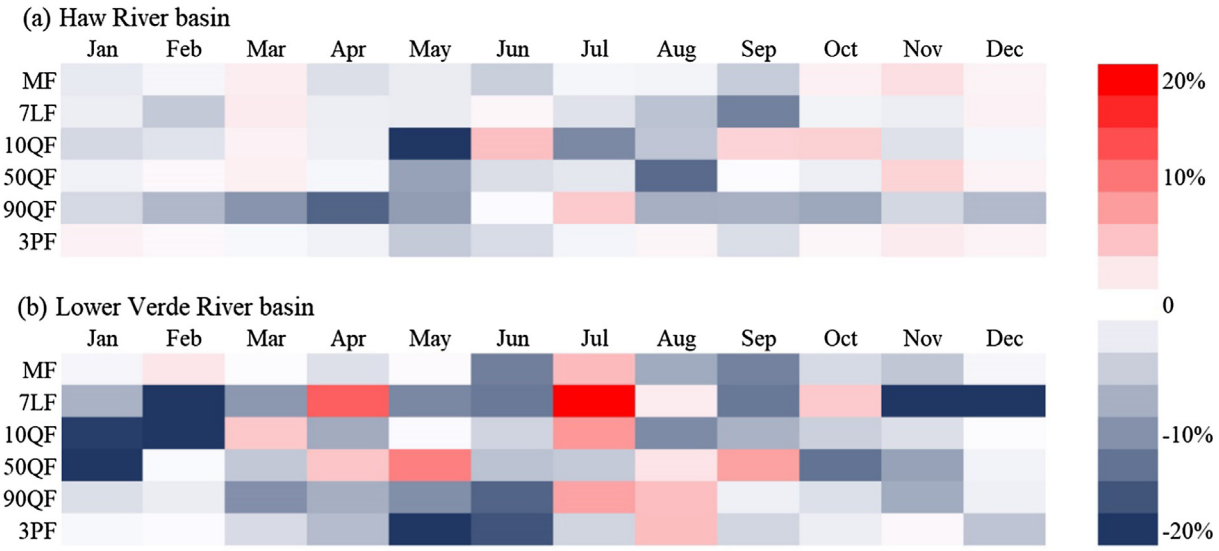

Fig. 5. Percent differences in RMSE of streamflow variables between Opt 1 and Opt 2 (i.e., (RMSE of Opt 1 – RMSE of Opt 2)/RMSE of Opt 1). MF: mean monthly streamflow, 7LF: mean monthly 7-day low streamflow, 10QF: 10 percentile monthly streamflow, 50QF: 50 percentile monthly streamflow, 90QF: 90 percentile monthly streamflow, and 3PF: mean monthly 3-day peak streamflow.

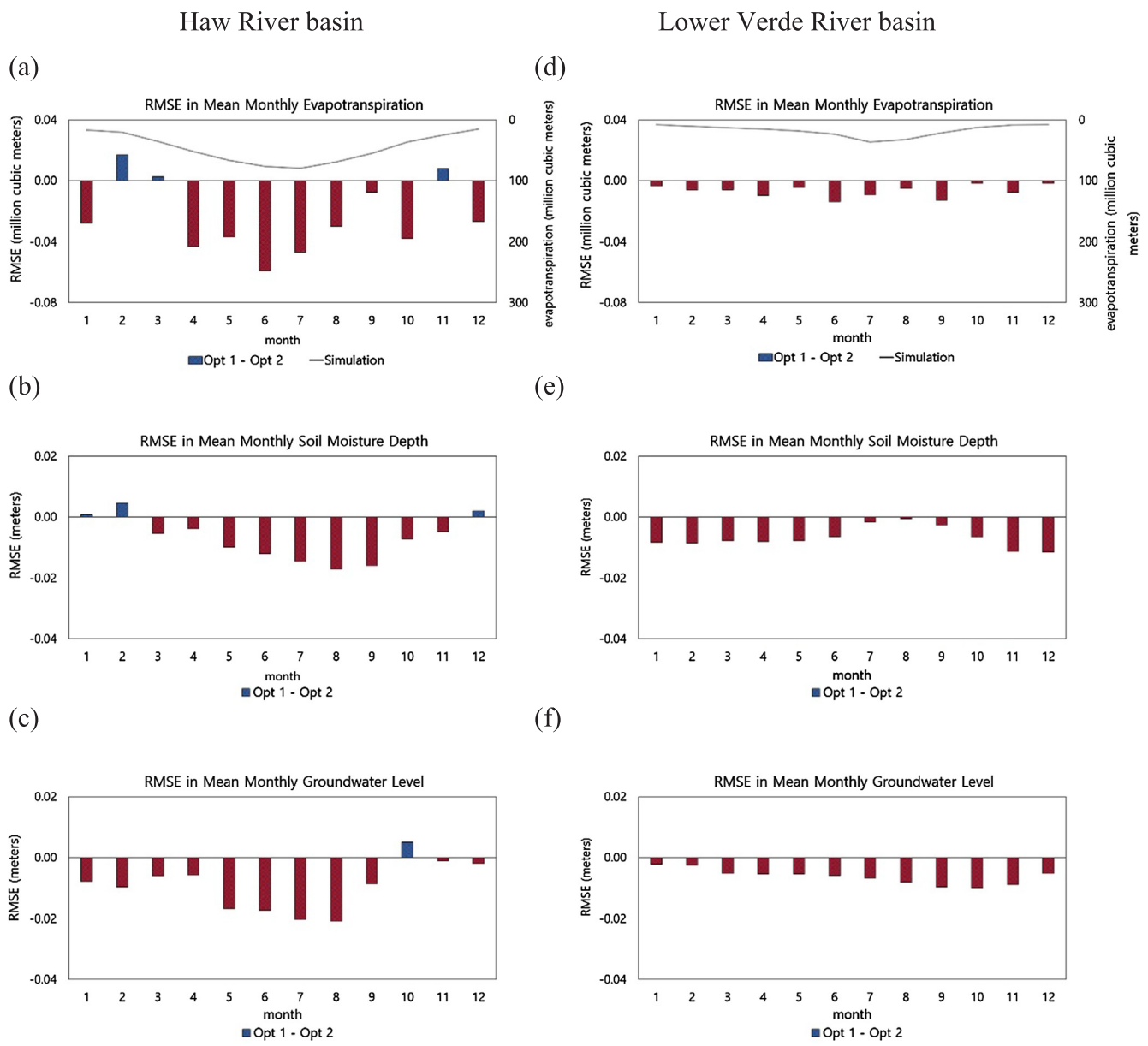

Fig. 6. Differences in RMSE of sub-surface hydrologic variables between Opt 1 and Opt 2 (i.e., RMSE of Opt 1 – RMSE of Opt 2). (a) Haw River basin – mean monthly evapotranspiration; (b) Haw River basin – mean monthly soil moisture depth; (c) Haw River basin – mean monthly groundwater level; (d) Lower Verde River basin – mean monthly evapotranspiration; (e) Lower Verde River basin – mean monthly soil moisture depth; and (f) Lower Verde River basin – mean monthly groundwater level.

evaluate the impact of near-term climate change on hydrologic variables (e.g., Seo et al., 2018c), using GCM forcings with biased P-T cross-correlation can cause adverse impacts on the hydrologic projections. Hence, we emphasize that inferences based on a bias-correction and downscaling schemes that do not reproduce the observed P-T cross-correlation should be interpreted carefully as the findings could be influenced by the pre-processing schemes. Previous studies suggest the necessity of multivariate techniques for bias-correction and statistical downscaling (He et al., 2012; Zhang and Georgakakos, 2012; Das Bhowmik et al., 2017) that can reproduce the joint dependency between P and T. Such multivariate bias-correction schemes can be considered for hydrologic projections particularly for basins that experience significant P-T cross-correlation.

In recent years, Abatzoglou and Brown (2012) proposed a multivariate downscaling approach MACA based on the constructed analog technique developed by Hidalgo et al. (2008). MACA performs bias-correction in GCM simulation by identifying the patterns between the GCM and the observed records. The concept of quantile mapping for univariate downscaling is extended by He et al. (2012) to simultaneously downscale P and T. Asynchronous Canonical Correlation Analysis (ACCA) can correct bias in multiple variables along with yielding the observed P-T cross-correlation in the bias-corrected products (Das Bhowmik et al., 2017). However, multivariate bias-correction techniques result in a trade-off between yielding the observed P-T cross-correlation and reproducing the temporal variability in P and T. Das Bhowmik et al. (2017) showed that even with the trade-off between the P-T cross-correlation and their variances, ACCA better reproduces the joint probability of occurrence of P and T. However, the current study did not consider the multivariate schemes as it would require a comparison between multivariate schemes to estimate the joint probability of occurrence of land-surface fluxes. One potential alternative is to use Regional Climate Model (RCM) outputs as inputs to the hydrologic model, provided the P-T cross-correlation from the RCM is within the sampling variability of the observed P-T cross-correlation.

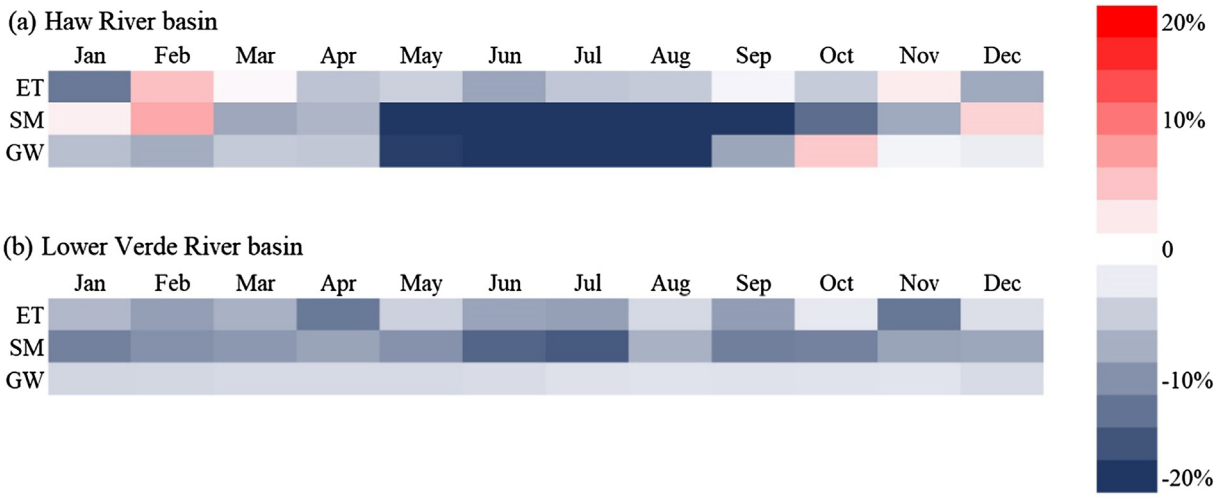

Fig. 7. Percent differences in RMSE of sub-surface hydrologic variables between Opt 1 and Opt 2 (i.e., (RMSE of Opt 1 – RMSE of Opt 2)/RMSE of Opt 1). ET: mean monthly evapotranspiration, SM: mean monthly soil moisture depth, and GW: mean monthly groundwater level.

Future extension of the current study will focus on understanding how multivariate bias-correction techniques influence hydrologic simulations. It would also be of interest to evaluate how climate forcings from univariate and multivariate bias-correction techniques reproduce the cross-correlation structure of land-surface fluxes. We expect that the performance of different pre-processing schemes could significantly vary, depending on basin's climate regime. For instance, if a robust P-T cross-correlation is witnessed in a basin, we presume that multivariate techniques (e.g., ACCA or multi-variate quantile mapping by He et al. (2012)) would likely produce an unbiased estimation of surface and sub-surface variables. However, if the river basin witnesses a high temporal variability in the P but statistically insignificant P-T cross-correlation, a traditional univariate linear bias-correction approach, like constructed analogues or quantile mapping, are expected to perform as efficiently as (or even better than) multivariate techniques, since univariate techniques better reproduce the variability in the forcings. Besides, it would be worthwhile to perform a further comparison between the impacts of 'bias in mean climate forcings' and 'bias in P-T cross-correlation' on the errors in hydrologic simulations. This investigation will have application in determining plausible GCMs for climate change impacts studies, as discussed in Seo and Kim (2018). It is also important to consider further improvements of multivariate pre-processing schemes so that they estimate the joint probability of occurrence of climate forcings along with reproducing the means and their standard deviations.

Acknowledgments

This research was supported in part by the National Science Foundation under grant number 1204368. Any opinions, findings, and conclusions or recommendations expressed in this material are those of the authors and do not necessarily reflect the views of the National Science Foundation.

Gridded observed precipitation and temperature data are available at Ed Maurer's webpage (http://www.engr.scu.edu/~emaurer/gridded_obs/index_gridded_obs.html). Streamflow and groundwater-level data for the target basins are available at USGS Water Data webpage (http://waterdata.usgs.gov/nwis). Watershed data sets – watershed boundary shapefiles, terrain data on digital elevation, and land cover classification data – are available at the USGS national map viewer and download platform (http://nationalmap.gov/viewer.html)

Appendix A. Supplementary data

Supplementary data to this article can be found online at https://doi.org/10.1016/j.jhydrol.2018.12.076.

Reference

Cai, W., Cowan, T., 2008. Evidence of impacts from rising temperature on inflows to the Murray-Darling Basin. Geophys. Res. Lett. 35 (7). https://doi.org/10.1029/2008GL033390.

Abatzoglou, J.T., Brown, T.J., 2012. A comparison of statistical downscaling methods suited for wildfire applications. Int. J. Climatol. 32, 772–780.

Chen, J., Li, C., Brissette, F.P., Chen, H., Wang, M., Essou, G.R., 2018. Impacts of correcting the inter-variable correlation of climate model outputs on hydrological modeling. J. Hydrol. (Amst.) 560, 326–341. https://doi.org/10.1016/J.JHYDROL.2018.03.040.

Choudhury, D., Sen Gupta, A., Sharma, A., Mehrotra, R., Sivakumar, B., 2017. An assessment of drift correction alternatives for CMIP5 decadal predictions. J. Geophys. Res. Atmos. 122 (19).

Das Bhowmik, R. 2016. Reducing Downscaling & Model Uncertainties in CMIP5 Decadal Hindcasts/Projections, Ph.D. dissertation, North Carolina State Univ. (Available at https://repository.lib.ncsu.edu/handle/1840.20/33329).

Das Bhowmik, R., Sankarasubramanian, A., Sinha, T., Mahinthakumar, G., Kunkel, K.E., 2017. Multivariate downscaling approach preserving cross-correlations across climate variable for projecting hydrologic fluxes. J. Hydrometeorol. https://doi.org/10.1175/JHM-D-16-0160.1.

He, X., Yang, Y., Zhang, J., 2012. Bivariate downscaling with asynchronous measurements. J. Agric. Biol. Environ. Stat. 17 (3), 476–489. https://doi.org/10.1007/s13253-012-0098-6.

Hidalgo, H., Dettinger, M.D., Cayan, D.R. 2008. Downscaling with constructed analogues – Daily precipitation and temperature fields over the United States: California Energy Commission Report CEC-500-2007-123, pp. 62.

Hosseinzadehtalaei, P., Tabari, H., Willems, P., 2017. Uncertainty assessment for climate change impact on intense precipitation: how many model runs do we need? Int. J. Climatol. 37 (S1), 1105–1117.

Hovenga, P.A., Wang, D., Medeiros, S.C., Hagen, S.C., Alizad, K., 2016. The response of runoff and sediment loading in the Apalachicola River, Florida to climate and land use land cover change. Earth's Future 4 (5), 124–142.

Huth, R., 1999. Statistical downscaling in Central Europe: evaluation of methods and potential predictors. Clim. Res. 13 (2), 91–101.

Ivanov, M.A., Kotlarski, S., 2017. Assessing distribution-based climate model bias correction methods over an alpine domain: added value and limitations. Int. J. Climatol. 37 (5), 2633–2653. https://doi.org/10.1002/joc.4870.

Johnson, F., Sharma, A., 2012. A nesting model for bias correction of variability at multiple time scales in general circulation model precipitation simulations. Water. Resour. Res. 48 (1).

Kormos, P.R., Luce, C.H., Wenger, S.J., Berghuijs, W.R., 2016. Trends and sensitivities of low streamflow extremes to discharge timing and magnitude in Pacific Northwest mountain streams. Water. Resour. Res. 52, 4990–5007. https://doi.org/10.1002/2015WR018125.

Kumar, M., 2009. Toward a Hydrologic Modeling System, Ph.D. thesis. Pennsylvania State Univ.

Liu, C., Allan, R.P., Huffman, G.J., 2012. Co-variation of temperature and precipitation in CMIP5 models and satellite observations. Geophys. Res. Lett. 39 (13). https://doi.org/10.1029/2012GL052093.

Maurer, E.P., Duffy, P.B., 2005. Uncertainty in projections of streamflow changes due to climate change in California. Geophys. Res. Lett. 32 (3). https://doi.org/10.1029/2004GL021462.

Maurer, E.P., Wood, A.W., Adam, J.C., Lettenmaier, D.P., Nijssen, B., 2002. A long-term hydrologically based dataset of land surface fluxes and states for the conterminous United States. J. Clim. 1993, 3237–3251. https://doi.org/10.1175/1520-0442(2002)015.

Mazrooei, A., Sinha, T., Sankarasubramanian, A., Kumar, S., Peters-Lidard, C., 2015. Decomposition of sources of errors in seasonal streamflow forecasting over the U.S. Sunbelt. J. Geophys. Res. Atmos. 120, 11809–11825. https://doi.org/10.1002/2015JD023687.

Prairie, J., Rajagopalan, B., Lall, U., Fulp, T., 2007. A stochastic nonparametric technique for space-time disaggregation of streamflows. Water. Resour. Res. 43, W03432. https://doi.org/10.1029/2005WR004721.

Qu, Y., Duffy, C.J., 2007. A semi discrete finite volume formulation for multiprocess watershed simulation. Water. Resour. Res. 43 (8). https://doi.org/10.1029/2006WR005752.

Reclamation. 2013. Downscaled CMIP3 and CMIP5 Climate Projections: Release of Downscaled CMIP5 Climate Projections, Comparison with Preceding Information, and Summary of User Needs. iv Downscaled CMIP3 and CMIP5 Climate and Hydrology Projections U.S. Department of the Interior, Bureau of Reclamation, Technical Service Center, Denver, Colorado, 116, [Available at http://gdodcp.ucllnl.org/downscaled_cmip_projections/techmemo/downscaled_c limate.pdf].

Sankarasubramanian, A., Lall, U., 2003. Flood quantiles and changing climate: Seasonal forecasts and causal relations. Water. Resour. Res. 39 (5) art.no.1134.

Sankarasubramanian, A., Vogel, R.M., 2003. Hydroclimatology of the continental United States. Geophys. Res. Lett. 30 (7). https://doi.org/10.1029/2002GL015937.

Sankarasubramanian, A., Vogel, R.M., Limbrunner, J.F., 2001. Climate elasticity of streamflow in the United States. Water. Resour. Res. 37 (6), 1771–1781. https://doi.org/10.1029/2000WR900330.

Seo, S.B., Sinha, T., Mahinthakumar, G., Sankarasubramanian, A., Kumar, M., 2016. Identification of dominant source of errors in developing streamflow and groundwater projections under near-term climate change. J. Geophys. Res. Atmos. 121. https://doi.org/10.1002/2016JD025138.

Seo, S.B., Mahinthakumar, G., Sankarasubramanian, A., Kumar, M., 2018a. Assessing the restoration time of surface water and groundwater systems under groundwater pumping. Stoch. Environ. Res. Risk. Assess. https://doi.org/10.1007/s00477-018-1570-9.

Seo, S.B., Mahinthakumar, G., Sankarasubramanian, A., Kumar, M., 2018b. Conjunctive management of surface water and groundwater resources under drought conditions using a fully-coupled hydrological model. J. Water. Res. Plan. Manage. 144 (9), 04018060.

Seo, S.B., Kim, Y.-O., Kim, Y., Eum, H.-I., 2018c. Selecting climate change scenarios for regional hydrologic impact studies based on climate extreme indices. Dynam. Clim 10.1007/s00382-018-4210-7.

Seo, S.B., Kim, Y.-O., 2018. Impact of spatial aggregation level of climate indicators on a national-level selection for representative climate change scenarios. Sustainability 10, 2409. https://doi.org/10.3390/su10072409.

Šraj, M., Viglione, A., Parajka, J., Blöschl, G., 2016. The influence of non-stationarity in extreme hydrological events on flood frequency estimation. J. Hydrol. Hydromech. 64 (4), 426–437.

Stoner, A.M.K., Hayhoe, K., Yang, X., Wuebbles, D.J., 2012. An asynchronous regional regression model for statistical downscaling of daily climate variables. Int. J. Climatol. 33, 2473–2494.

Taylor, K.E., Stouffer, R.J., Meehl, G.A., 2012. An overview of CMIP5 and the experiment design. B. Am. Meteorol. Soc. 93, 485–498.

Trenberth, K.E., Shea, D.J., 2005. Relationships between precipitation and surface temperature. Geophys. Res. Lett. 32 (14), 1–4. https://doi.org/10.1029/2005GL022760.

USGS Water Data webpage. 2015. “USGS Water Data for the Nation (Available at http://waterdata.usgs.gov/nwis/) (retrieved on 5.03.15).

van Werkhoven, K., Wagener, T., Reed, P., Tang, Y., 2008. Rainfall characteristics define the value of streamflow observations for distributed watershed model identification. Geophys. Res. Lett. 35 (11). https://doi.org/10.1029/2008GL034162.

Vano, J.A., Das, T., Lettenmaier, D.P., 2012. Hydrologic sensitivities of Colorado River runoff to changes in precipitation and temperature. J. Hydrol. 13 (3), 932–949. https://doi.org/10.1175/JHM-D-11-069.1.

Vogel, R.M., Sankarasubramanian, A., 2000. Spatial scaling properties of annual streamflow in the United States. Hydrolog. Sci. J. 45 (3), 465–476. https://doi.org/10.1080/02626660009492342.

Wilcke, R.A.I., Mendlik, T., Gobiet, A., 2013. Multi-variable error correction of regional climate models. Clim. Change. 120 (4), 871–887.

Wilks, D.S., Wilby, R.L., 1999. The weather generation game: a review of stochastic weather models. Prog. Phys. Geogr. 23 (3), 329–357.

Wood, A.W., Leung, L.R., Sridhar, V., Lettenmaier, D.P., 2004. Hydrologic implications of dynamical and statistical approaches to downscaling climate model outputs. Clim. Change. 62, 189–216.

Zhang, F., Georgakakos, A.P., 2012. Joint variable spatial downscaling. Clim. Change. 111 (3), 945–972. https://doi.org/10.1007/s10584-011-0167-9.

Zhang, X., Tang, Q., Zhang, X., Lettenmaier, D.P., 2014. Runoff sensitivity to global mean temperature change in the CMIP5 Models. Geophys. Res. Lett. 41 (15), 5492–5498. https://doi.org/10.1002/2014GL060382.

Zhao, W.N., Khalil, M.a.K., 1993. The relationship between precipitation and temperature over the contiguous United-States. J. Clim. 6 (6), 1232–1236. https://doi.org/10.1175/1520-0442(1993) 006.